Electronic Supplementary Material (ESI) for RSC Advances.

Supporting Information for

Ionothermally Synthesized Hierarchical Porous Schiff-Base-Type Polymeric Networks with Ultrahigh Specific Surface Area for Supercapacitors

Yuhang Zhao,[a] Ping Liu,[b*] Xiaodong Zhuang, Dongqing Wu,[b] Fan Zhang and Yuezeng Su[c*]

[a.] School of Aeronautics and Astronautics, Shanghai Jiao Tong University, 800 Dongchuan RD, Shanghai 200240, P. R. China.

[b.] School of Chemistry and Chemical Engineering, Shanghai Jiao Tong University, 800 Dongchuan RD, Shanghai 200240, P. R. China. ***E-mail: liupingsjj@sjtu.edu.cn.***

[c.] School of Electronic Information and Electrical Engineering, Shanghai Jiao Tong University, 800 Dongchuan RD, Shanghai 200240, P. R. China. ***E-mail: yzsu@sjtu.edu.cn.***

Experimental Section:

Materials

Organic solvents were purified, dried, and distilled under dry nitrogen. All the chemicals were purchased from Aladdin Reagent (Shanghai) and used without further purification.

Preparation of HPPNs

In order to ensure the basic structure of this material resemble that shown in Scheme 1. The polymerization was carried out at a moderate temperature of 400°C for varied reaction time. Melamine (63mg, 0.5mmol), anthraquinone (156mg, 0.75mmol) and aluminium chloride (666.7 mg, 5mmol) were mixed in a 25 mL pyrex ampoule evacuated by vacuum, sealed and heated at 400°C for 15, 30, 60 and 90 hours, respectively. The ampoule was then cooled down to room temperature and the resulting black tablet was grounded in a mortar, washed thoroughly with aqueous hydrochloric acid solution (1M), deionized water, tetrahydrofuran (THF), N,N-dimethylformamide (DMF), alcohol upon sonication, and then dried under vacuum at 100°C for 24h to give HPPN-400-t (t: 15, 30, 60 and 90) as black powder. In order to investigate the temperature effect on the polymeric structure of polymers, a serious of HPPN-Ts (T: 300, 400, 500 and 600) samples were fabricated through 15 hours polymerization at different temperature from 300, 400, 500 to 600°C in the same way as described above. They are designated as HPPN-300, HPPN-400, HPPN-500 and HPPN-600.[1-3]

Characterization

FT-IR spectra were recorded on a Spectrum 100 (Perkin Elmer, Inc., USA) spectrometer. The morphology and elemental mapping information were obtained on a scanning electron microscopy (SEM, Sirion 200, 25kV) and transmission electron microscopy (TEM, JEOL JEM-2010, 200kV). X-ray diffraction (XRD) measurements were performed on a D/max-2200/PC (Rigaku Corporation, Japan) using Cu (40kV, 30mA) radiation. Raman spectra were recorded on a Senterra R200-L (Bruker Optics) using a 5 mW Ar-ion laser at 532 nm excitation. Solid-state ^{13}C CP-MAS NMR measurements were performed on a Bruker Avance III 400MHz NMR spectrometer at a MAS rate of 5 kHz and a CP contact time of 1 ms. N_2 adsorption-desorption isotherms at 77 K were determined by using a Micromeritics ASAP 2010 instrument. The Brunauer–Emmett–Teller (BET) method and density functional theory (DFT) pore model were utilized to calculate the specific surface area and pore size distribution. Thermogravimetric analysis (TGA) were performed on a Q5000IR (TA Instruments, USA) thermogravimetric analyzer at a heating rate of 20°C min^{-1} under nitrogen atmosphere. X-ray photoelectron spectroscopy (XPS) measurements were carried out on an AXIS Ultra DLD system from Kratos with Al Kα radiation as the X-ray source.

Electrochemical measurements

Electrochemical measurements were performed on CHI 660e workstation (Chenhua, Shanghai). A conventional cell with a three-electrode configuration was employed to test the electrochemical performance. Working electrode was prepared by mixing HPPNs with carbon black (Mitsubishi Chemicals, Inc.) and poly-tetrafluoroethylene (PTFE) binder in a weight ratio of 7:2:1. The experiments were carried out at room temperature in a 1M H_2SO_4 solution with a platinum filament as counter electrode and an Ag/AgCl electrode as reference electrode.

In the case of all-solid-state supercapacitors (ASSSs), gel-like electrolyte was first fabricated by mixing H_2SO_4 (6g) and PVA (6g) in deionized water (60mL) and thus heated up to 85℃ under vigorous stirring for about 3 hours until the solution became clear. Two slices of stainless steel mesh were painted with the active material, and then immersed in the PVA/H_2SO_4 electrolyte. The resulting electrolyte-filled electrodes were solidified overnight at room temperature. Finally, as-prepared two electrodes were separated by a membrane and then symmetrically face to face integrated into one ASSS.

Cyclic voltammetric measurements were recorded from -0.3 to 0.7 V at a scan rate from 5 to 100 mV s^{-1}. Galvanostatic charge-discharge measurements were performed at different current densities in voltage from -0.3 to 0.7V. Electrochemical impedance spectroscopic (EIS) were recorded under open circuit potential in an AC frequency range from 100000 to 0.01 Hz.

The specific capacitance (C, F g^{-1}) of an electrode was calculated from the slope of discharge curve by using the equation of $C = I \times t / (V \times m)$, where I (A) is the discharge current, V (V) is the discharge voltage, t (s) is the discharge time, and m (g) is the mass of HHPPNs in the electrode.[4]

The energy density (E) of the two-electrode system was calculated from the discharge profiles by using the following equation: $E= 0.5\Delta V^2/3.6$, where E (Wh kg^{-1}) is the energy density, C (F g^{-1}) is the specific capacitance of the active material and ΔV (V) is the discharge voltage range. With a factor 3.6, the energy density is converted from J g^{-1} to Wh kg^{-1}. [5]

The power density (P) of the two-electrode system was calculated as follows: $P= E\times3600/\Delta t$ where P (W kg^{-1}) is the power density, and E (Wh kg^{-1}) and Δt (s) are the energy density and discharge time, respectively. [5]

Supplementary Figures

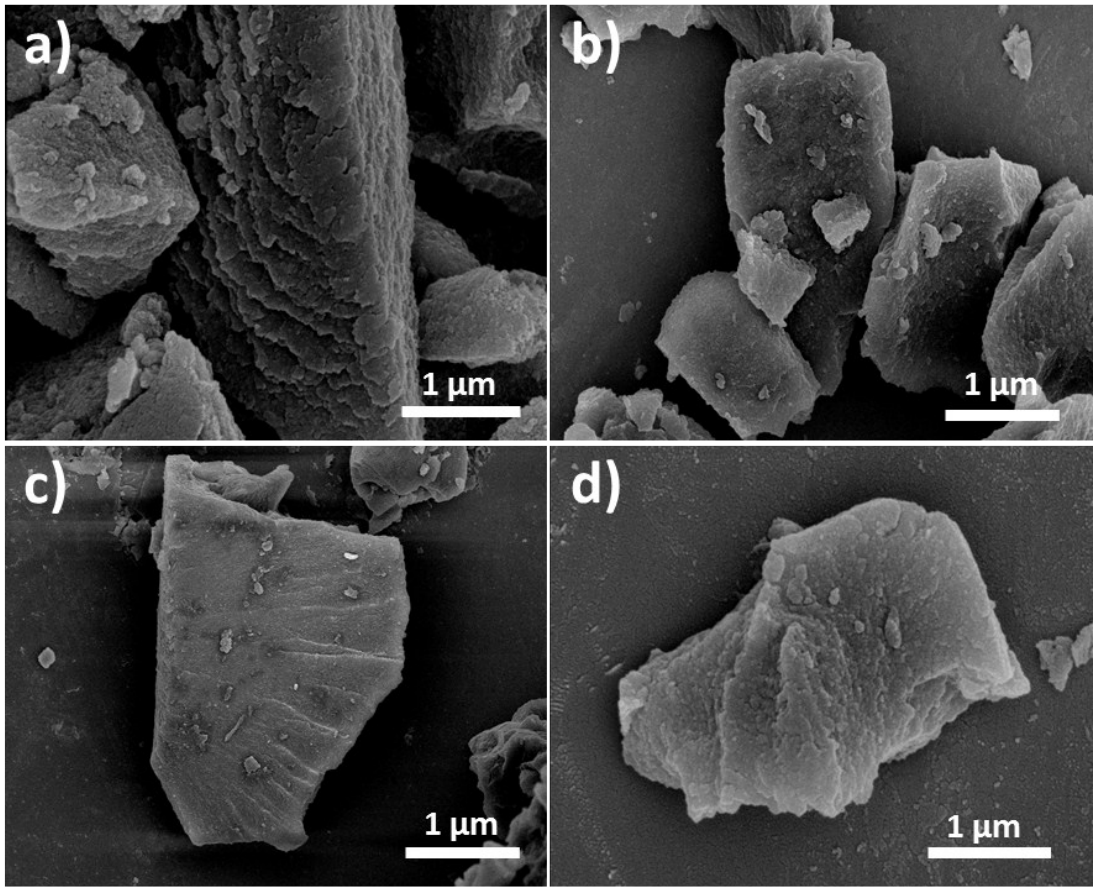

Figure S1. SEM images of a) HPPN-300, b) HPPN-400, c) HPPN-500, d) HPPN-600, respectively.

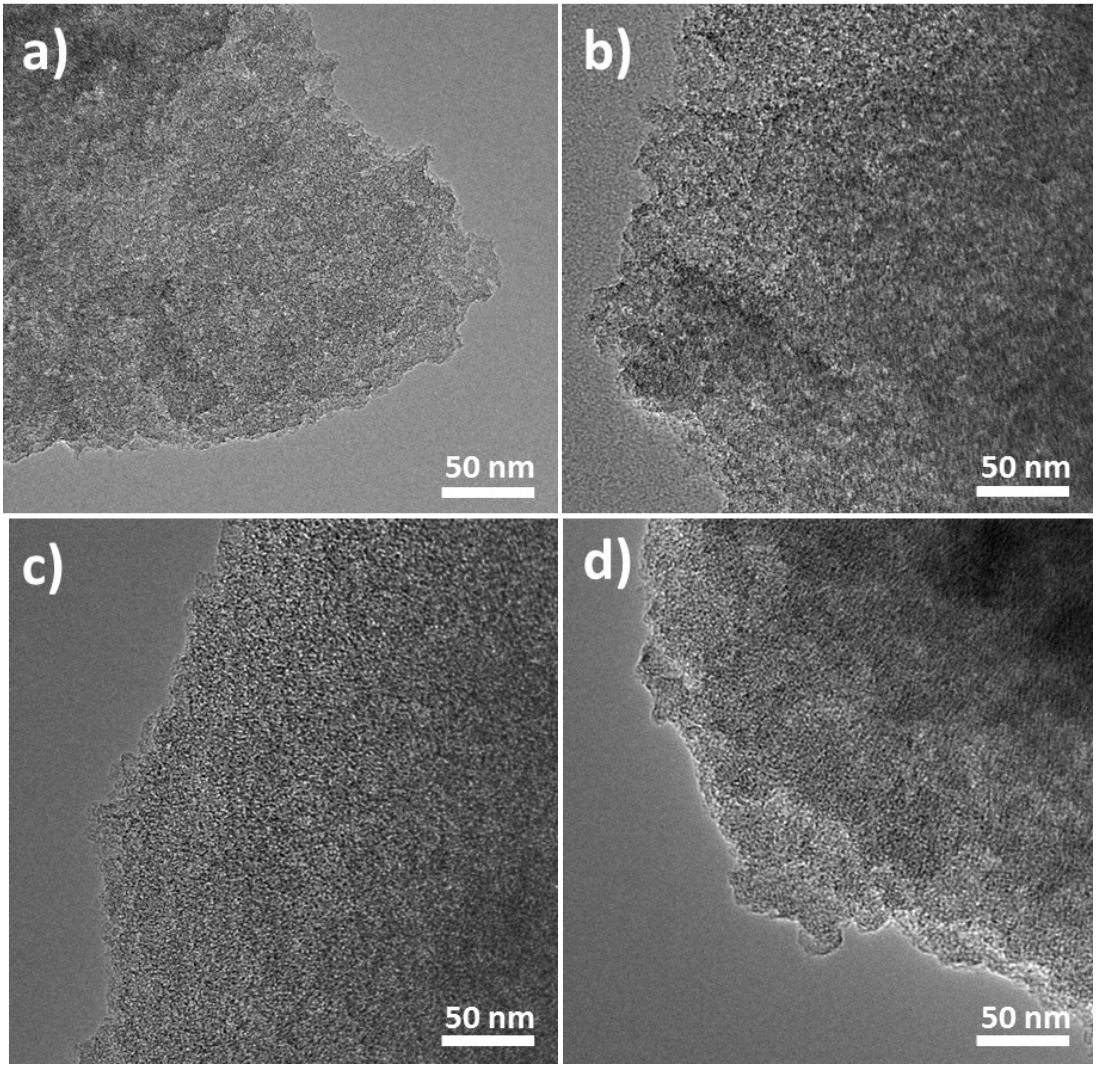

Figure S2. TEM images of a) HPPN-300, b) HPPN-400, c) HPPN-500 and d) HPPN-600.

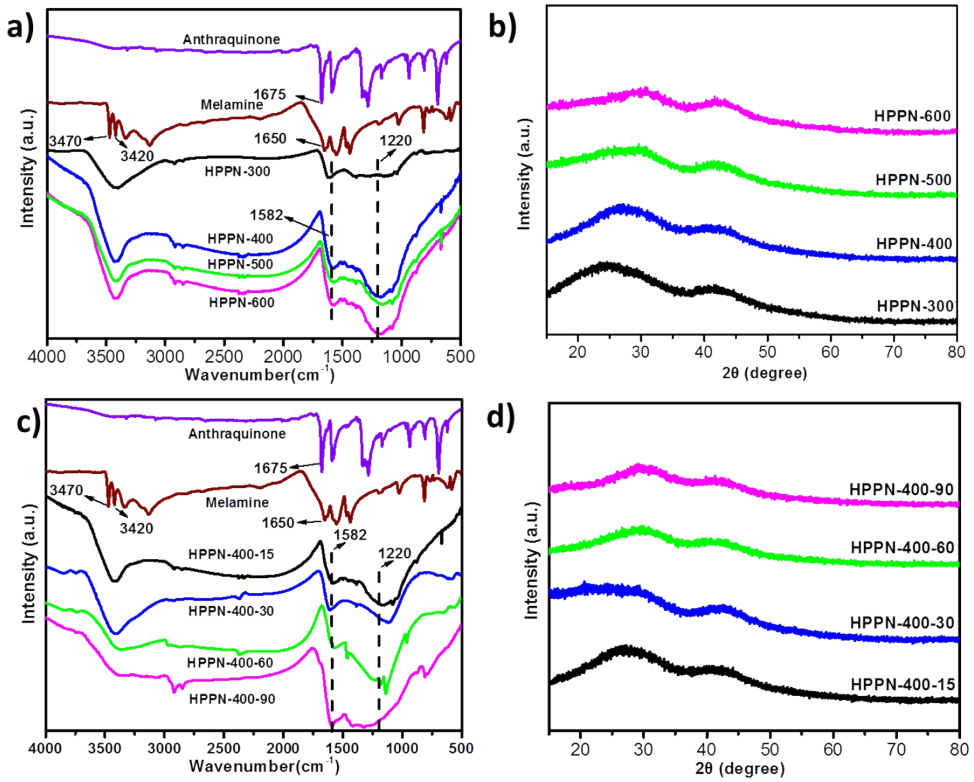

Figure S3. (a, c) FT-IR spectra and (b, d) X-ray powder diffraction patterns of HPPNs.

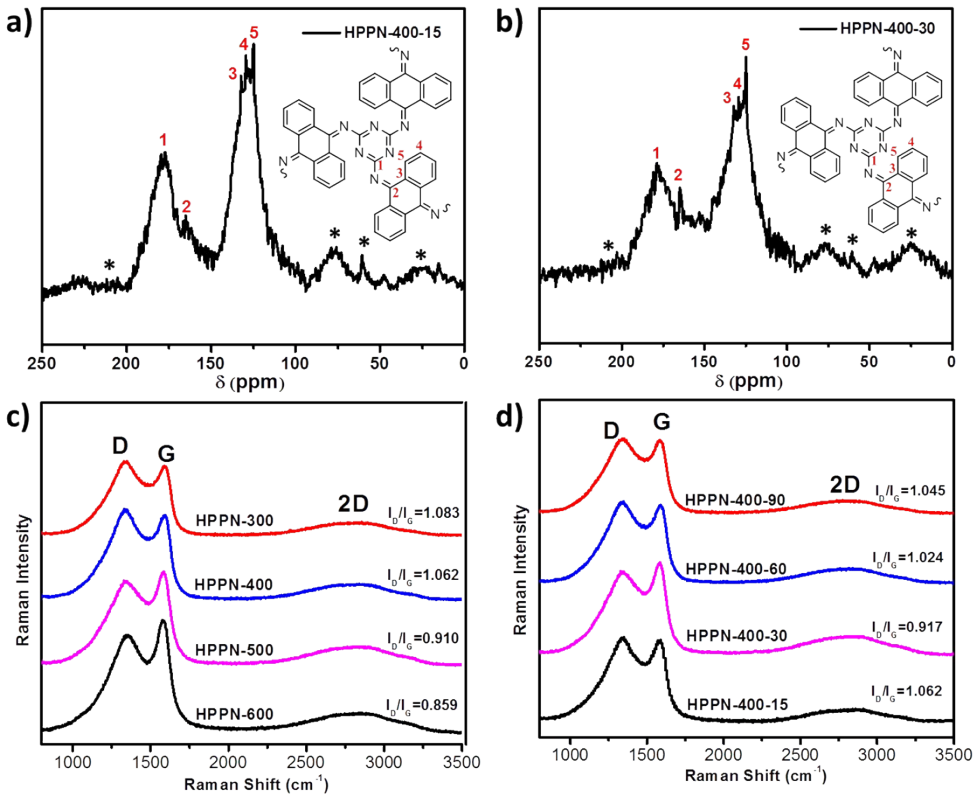

Figure S4. Solid-state ^{13}C CP-MAS NMR spectra of a) HPPN-400-15 and b) HPPN-400-30 and the signal assignments (*side peaks); Raman spectra of c) HPPN-T (T: 300, 400, 500 and 600) and d) HPPN-400-t (t: 15, 30, 60 and 90).

In ^{13}C CM-MAS NMR spectra, the peak at 177 ppm can be assigned to the carbon atoms in the triazine ring, while the signal located at 164 ppm might originate from the carbon atoms, constituting imine linkage, in the anthracene. The signals at 132, 129 and 124 ppm belong to the three kinds of carbon atoms of the anthracene phenyl edges, respectively.[1, 6] Consequently, it is experimentally confirmed that five kinds of carbons exist in HPPNs. In Raman spectra, the two prominent peaks at around 1340 and 1590 cm^{-1}were observed which correspond to the D (disordered) and G (order) bands of carbon, respectively. The I_D/I_G ratios of HPPN-T (T: 300, 400, 500 and 600) tend to decrease greatly with the rising of temperature from 300 to 600℃. The lowest I_D/I_G ratio of HPAP-600 (0.85) indicates a remarkable degree of graphitization of this carbonized polymeric network at 600℃.[7, 8] The fact is in line with the conclusion from quantitative analysis for the quaternary N content in XPS of HPPN-T. The I_D/I_G ratio for HPPN-400-t (t: 15, 30) tends o decrease from 1.062 to 0.917 when the polymerization time was prolonged from 15 hours to 30 hours; which means increased graphitization degree. Then the I_D/I_G ratio rises to 1.024 for HPPN-400-60 and 1.045 for HPPN-400-90 when the polymerization time was prolonged to 60 and 90 hours during synthetic processes; which suggests a decreasing graphitization

degree. These conclusion were in accord with the analyses from the XPS spectra of HPPN-400-ts (t: 15, 30, 60 and 90).

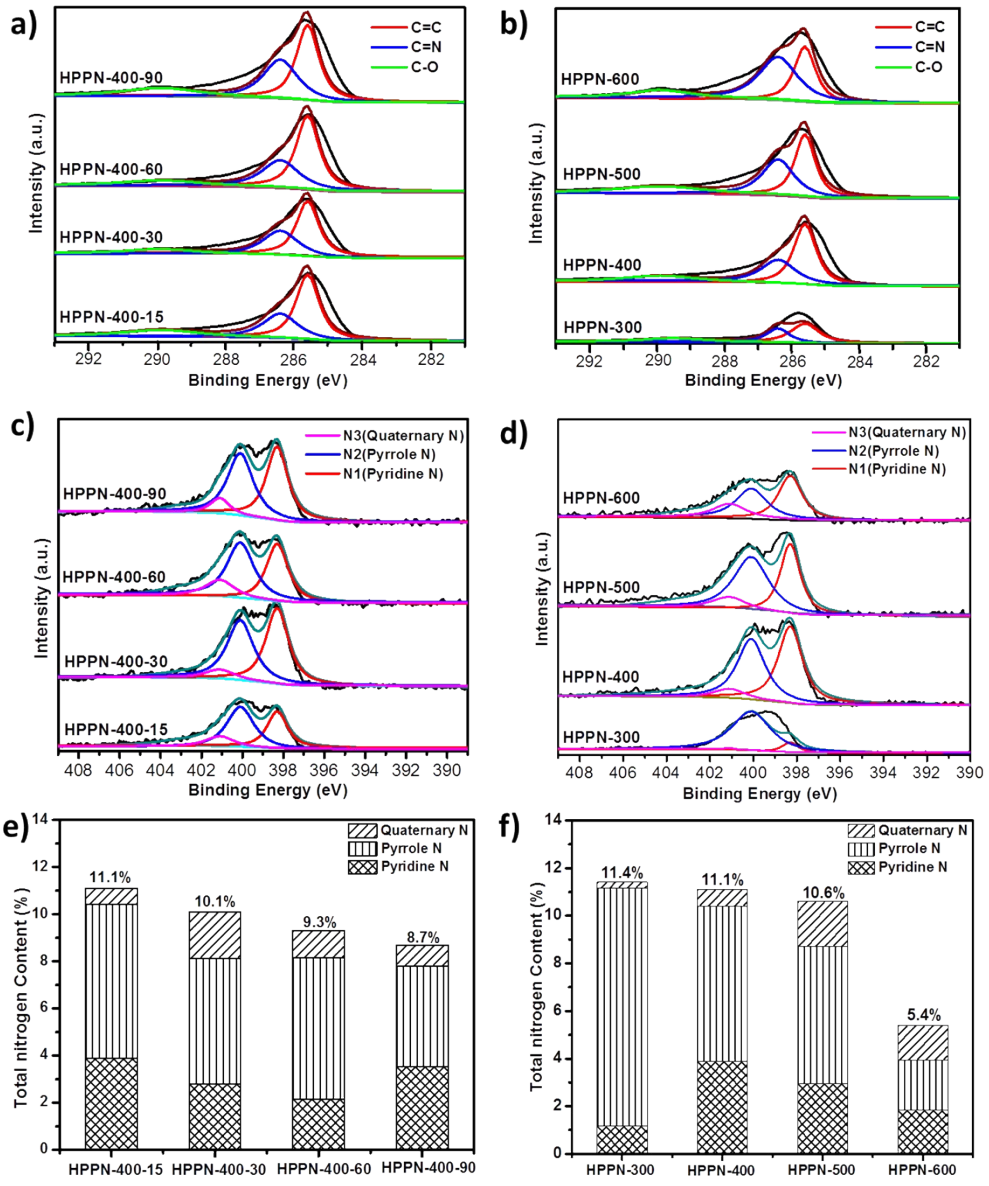

Figure S5. (a, b) high-resolution XPS C1s spectra, (c, d) high-resolution XPS N1s spectra of HPPNs, (e, f) atomic percentage of three nitrogen species of HPPNs derived from XPS analysis.

Table S1: Results of XPS analysis on element content and diversified nitrogen proportion

Sample	C	N	O	Pyridine N(%)	Pyrrole N(%)	Quaternary N(%)
HPPN-300	82.0	11.4	6.6	10.2	89.0	0.8
HPPN-400	80.6	11.1	8.3	35.0	58.8	6.2
HPPN-500	82.4	10.6	7.0	27.9	54.2	17.9
HPPN-600	78.9	5.4	15.7	33.9	38.9	27.2
HPPN-400-30	78.6	10.1	11.3	27.8	52.8	19.4
HPPN-400-60	79.2	9.3	11.5	23.2	64.5	12.3
HPPN-400-90	83.6	8.7	7.7	40.7	49.1	10.2

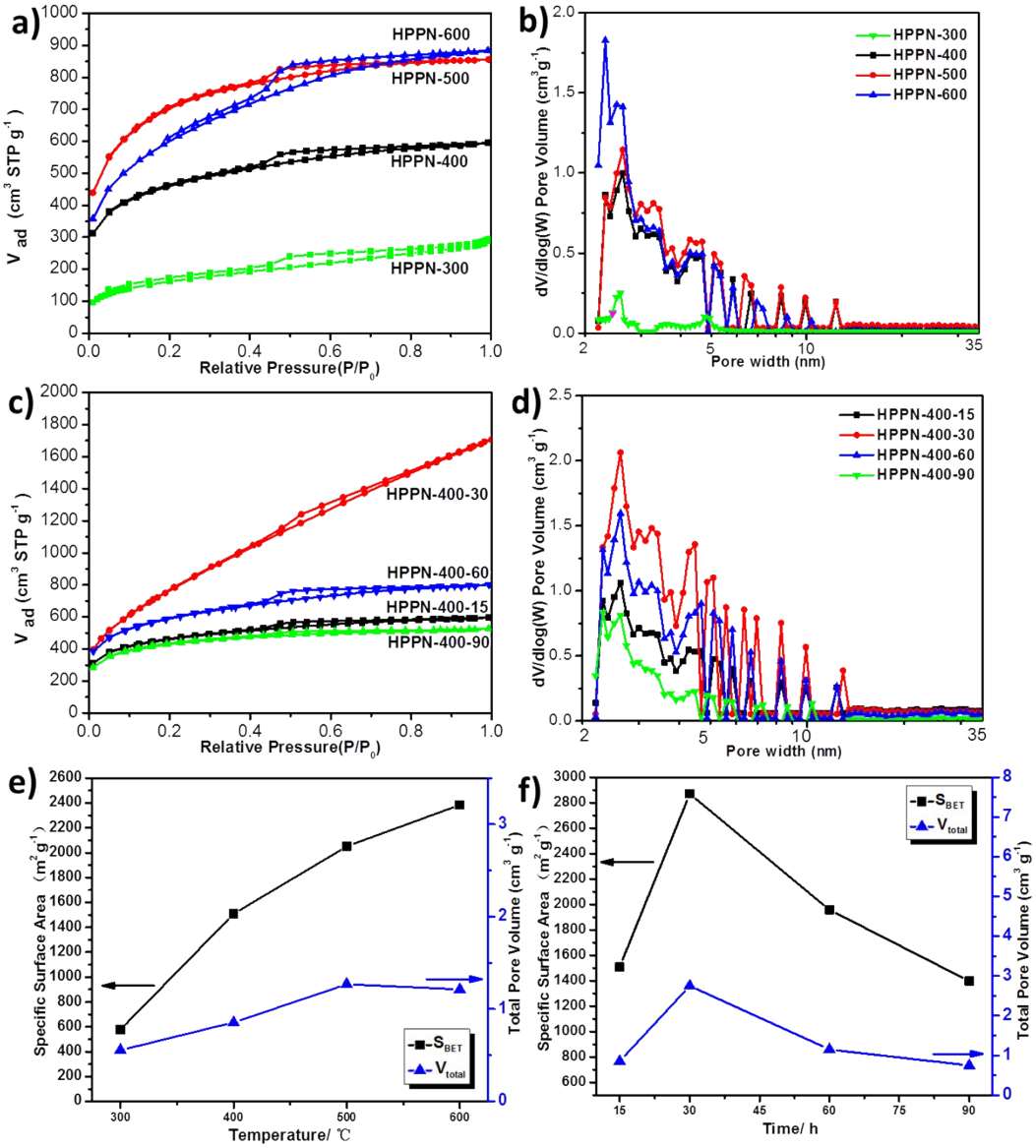

Figure S6. (a, c) Nitrogen adsorption/desorption isotherms, (b, d) pore size distribution calculated by NL-DFT method of HPPNs. The plots of the BET specific surface area and total pore volume versus e) synthesis temperature from 300, 400 500 to 600°C for HPPN-Ts (T: 300, 400, 500 and 600) and f) synthesis time from 15, 30 60 to 90 hours at 400 °C for HPPN-400-ts (t: 15, 30, 60 and 90).

Table S2. Nitrogen physisorption properties of HPPNs.

Sample	S_{BET}[a](m^2 g^{-1})	V_{total}[b](cm^3 g^{-1})	V_{micro}[c](cm^3 g^{-1})	D_{av}[d](nm)
HPPN-300	578	0.556	0.352	1.96
HPPN-400	1508	0.855	0.602	1.45
HPPN-500	2051	1.268	0.689	1.40
HPPN-600	2384	1.211	0.903	1.25
HPPN-400-30	2870	2.750	0.624	1.97
HPPN-400-60	1958	1.149	0.744	1.48
HPPN-400-90	1397	0.746	0.565	1.83

[a] Specific surface area calculated by BET method. [b]Total pore volume. [c]Microporous pore volume. [d]Average pore size based on the adsorption isotherms.

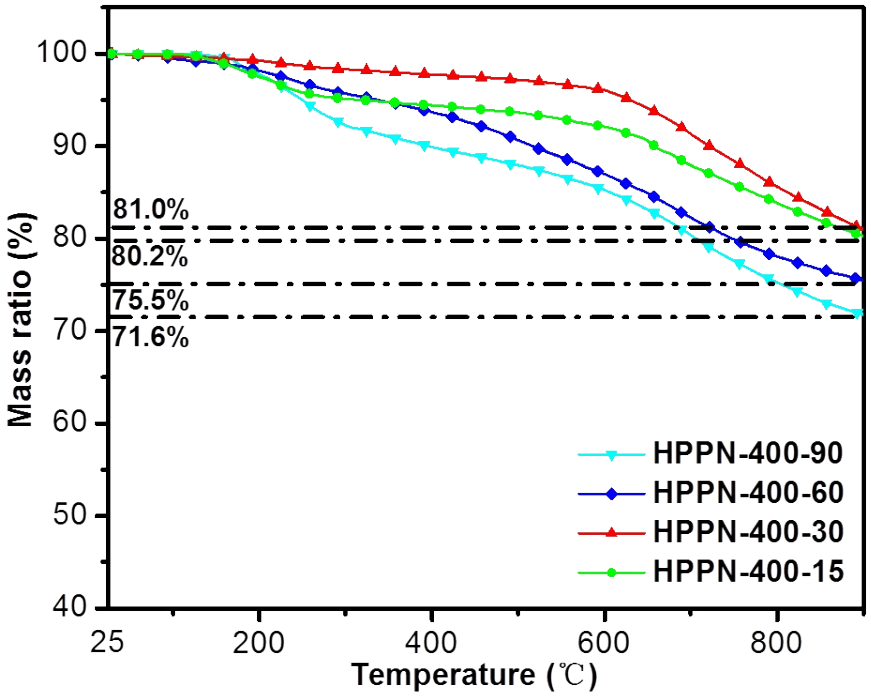

Figure S7. Thermogravimetric analysis (TGA) of HPPN-400-ts (t: 15, 30, 60 and 90).

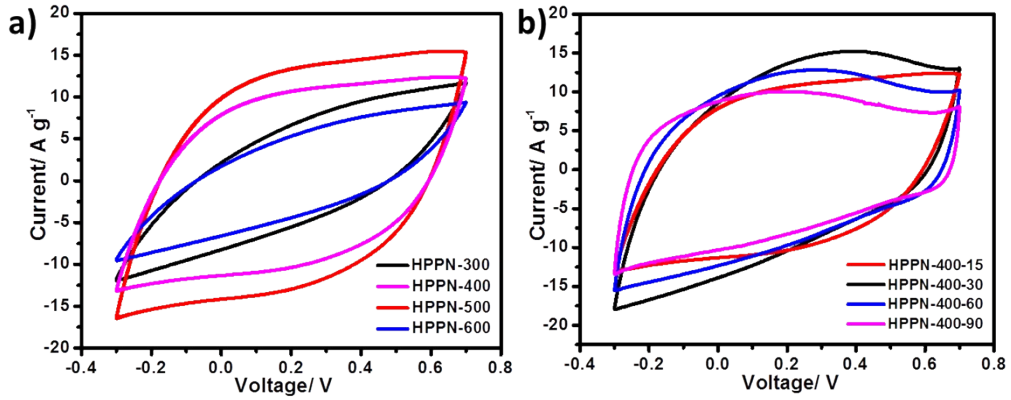

Figure S8. CV curves of a) HPPN-Ts (T: 300, 400,500 and 600) and b) HPPN-400-ts (t: 15, 30, 60 and 90) at the scan rate of 100 mV s^{-1}.

Table S3. **Specific capacitance (F g^{-1}) of HPPNs at different current densities.**

Current density(A g^{-1})	0.1	0.2	0.5	1	2	5	10
HPPN-300	185.8	166.6	148.7	138.6	130.8	118.0	104.0
HPPN-400	231.8	206.8	194.7	160.8	149.5	130.7	111.0
HPPN-500	251.8	228.4	202.5	183.5	163.0	125.0	85.0
HPPN-600	163.7	146.2	132.7	124.2	115.2	98.5	77.0
HPPN-400-30	312.7	253.2	214.4	193.8	166.8	140.2	129.6
HPPN-400-60	232.7	211.4	183.6	172.7	152.0	133.0	112.0
HPPN-400-90	235.0	199.8	180.9	168.7	141.2	116.5	97.0

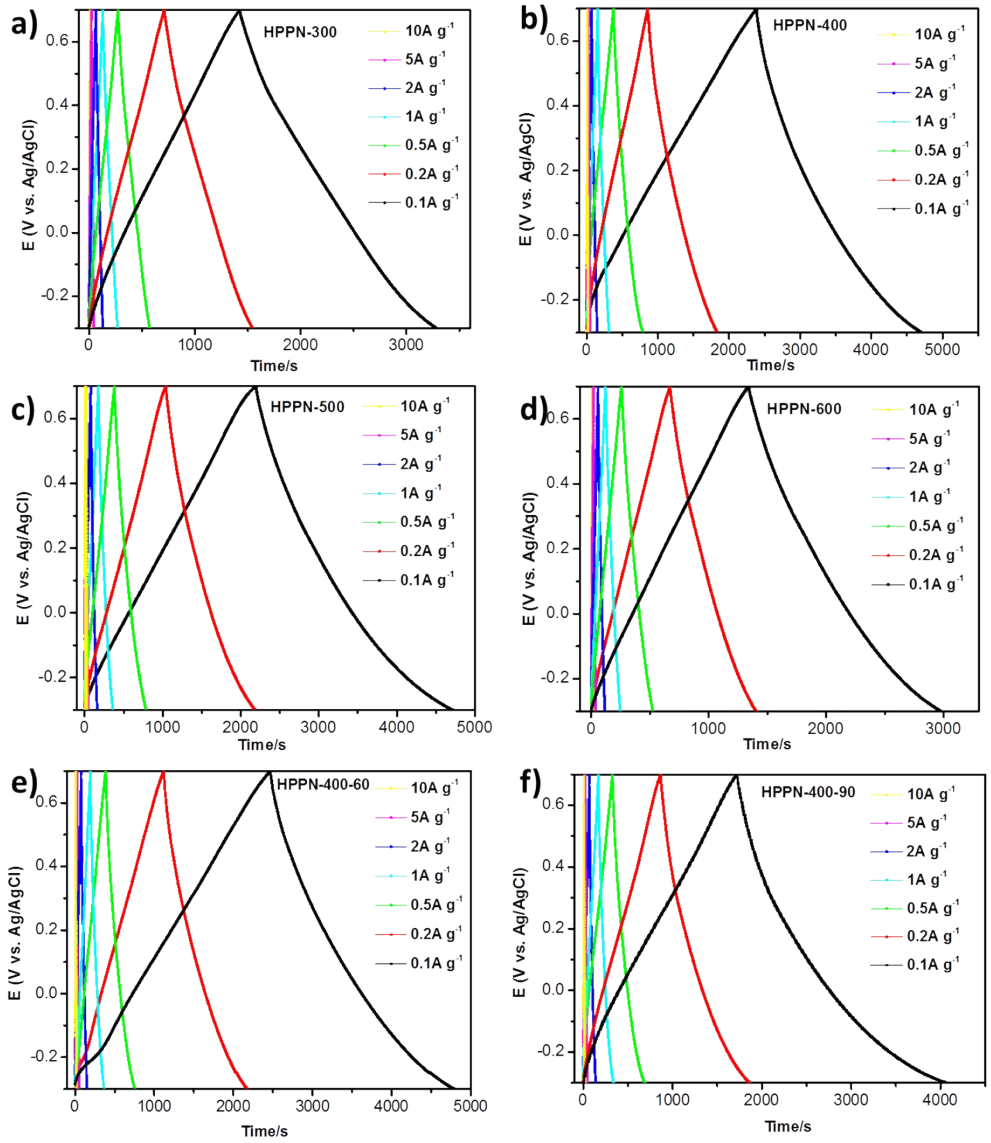

Figure S9. Charge and discharge curves of HPPNs at different current densities.

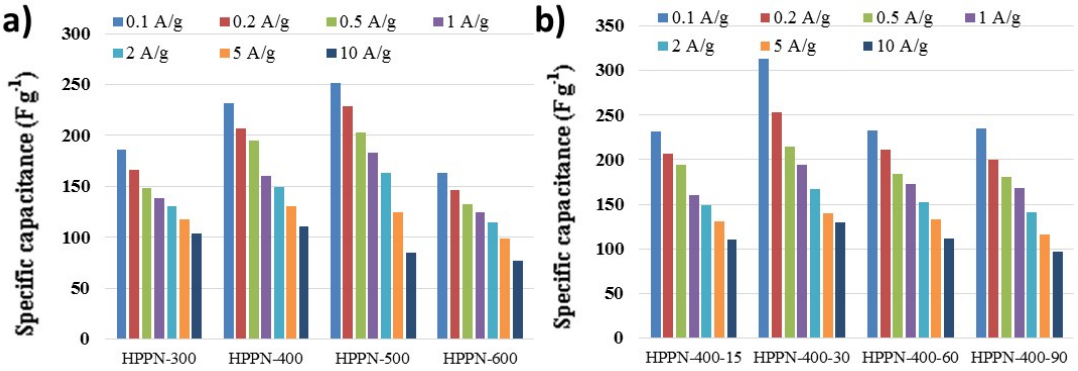

Figure S10. Specific capacitance (F g^{-1}) of a) HPPN-Ts (T: 300, 400,500 and 600) and b) HPPN-400-ts (t: 15, 30, 60 and 90) at different current densities (A g^{-1}).

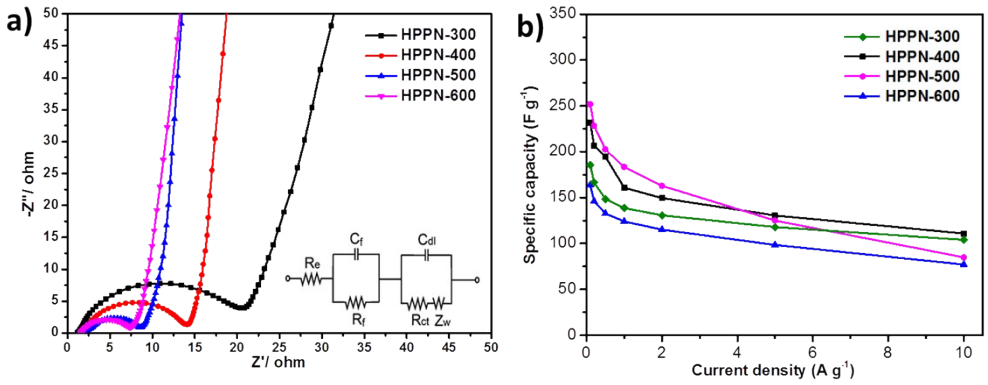

Figure S11. a) EIS plots of HPPN-Ts (T: 300, 400,500 and 600), the inset is the equivalent circuit of HPPNs based supercapacitors**;** b) Specific capacitance (F g^{-1}) of HPPN-Ts (T: 300, 400,500 and 600) at different current densities.

Table S4: Specific capacitance, energy density and power density of PAP-400-30 based ASSS device.

Current density (A g^{-1})	**0.1**	**0.2**	**0.5**	**1**	**2**	**5**	**10**
Specific capacitance (F g^{-1})	**96.8**	**93.1**	**90.1**	**85.4**	**78.6**	**63.0**	**58.0**
Energy density (Wh kg^{-1})	**13.4**	**12.9**	**12.5**	**11.9**	**10.9**	**8.8**	**8.1**
Power density (W kg^{-1})	**49.8**	**99.8**	**249.7**	**501.6**	**998.5**	**2514.3**	**5027.6**

Table S5: Comparison of gravimetric capacitances with carbon-based porous materials as electrodes of supercapacitors in previous reports.

Sample names	S_{BET} (m^2 g^{-1})	Condition	electrolyte	C_g (F g^{-1})	Refs
HPPN-400-30	2870	0.1 (A g^{-1})	1M H_2SO_4	312.7	This work
WDPC-1	818	1 (A g^{-1})	1M H_2SO_4	145	[4]
PGF	242	0.2 (A g^{-1})	6M KOH	237	[5]
Reduced graphene hydrogels	152	0.3 (A g^{-1})	6M KOH	230.4	[7]
JNC-1	2545	0.1 (A g^{-1})	1M H_2SO_4	292	[8]
HPHCMs	353	5 (mA cm^{-2})	2M KOH	278	[9]
N-doped graphene	-	1 (A g^{-1})	1M H_2SO_4	246.4	[10]
PCS	2500	0.5 (A g^{-1})	2M KOH	196	[11]
GC-10	998.7	1 (A g^{-1})	6M KOH	178.1	[12]
Graphene-PCs	-	0.2 (A g^{-1})	6M KOH	183	[13]
N-doped carbon spheres	1126	0.2 (A g^{-1})	6M KOH	247	[14]
Hierarchical porous carbons	759	0.2 (A g^{-1})	5M KOH	170	[15]
3D N-doped carbons	1408	1 (A g^{-1})	1M H_2SO_4	167	[16]
GPCs-800	-	5 (mV s^{-1})	1M H_2SO_4	298	[17]
Activated carbon aerogel	1935	0.125 (A g^{-1})	1M H_2SO_4	220	[18]
3D graphene-based frameworks	295	10 (mV s^{-1})	1M H_2SO_4	176	[19]

References

1 Y. Kou, Y. Xu, Z. Guo and D. Jiang, *Angew. Chem. Int. Ed.*, 2011, **50**, 8753-8757.

2. A. Thomas, *Angew. Chem.Int. Ed.*, 2010, **49**, 8328-8344.

3. Y. Su, Y. Liu, P. Liu, D. Wu, X. Zhuang, F. Zhang and X. Feng, *Angew. Chem. Int. Ed.*, 2015, **54**, 1812-1816.

4. D. K. Singh, K. S. Krishna, S. Harish, S. Sampath and M. Eswaramoorthy, *Angew. Chem. Int. Ed.*, 2016, **55**, 2032-2036.

5. D. Li, C. Yu, M. Wang, Y. Zhang and C. Pan, *RSC Adv.*, 2014, **4**, 55394-55399.

6. W. Zhao, S. Han, X. Zhuang, F. Zhang, Y. Mai and X. Feng, *J. Mater. Chem. A*, 2015, **3**, 23352-23359.

7. M. Jiang, J. L. Zhang, F. Qiao, R.-Y. Zhang, L.-B. Xing, J. Zhou, H. Cui and S. Zhuo, *RSC Adv.*, 2016, **6**, 48276-48282.

8. B. Lu, L. Hu, H. Yin, W. Xiao and D. Wang, *RSC Adv.*, 2016, **6**, 106485-106490.

9. F. Ran, X. Zhang, Y. Liu, K. Shen, X. Niu, Y. Tan, L. Kong, L. Kang, C. Xu and S. Chen, *RSC Adv.*, 2015, **5**, 87077-87083.

10. K. Yuan, Y. Xu, J. Uihlein, G. Brunklaus, L. Shi, R. Heiderhoff, M. Que, M. Forster, T. Chasse, T. Pichler, T. Riedl, Y. Chen and U. Scherf, *Adv. Mater.*, 2015, **27**, 6714-6721.

11. B. Chang, Y. Wang, K. Pei, S. Yang and X. Dong, *RSC Adv.*, 2014, **4**, 40546-40552.

12. Y. Zhang, W. Fan, Y. Huang, C. Zhang and T. Liu, *RSC Adv.*, 2015, **5**, 1301-1308.

13. H. Ren, J. Zhu, Y. Bi, Y. Xu and L. Zhang, *RSC Adv.*, 2016, **6**, 89140-89147.

14. Z. Sun, S. Shen, L. Ma, D. Mao and G. Lu, *RSC Adv.*, 2016, **6**, 104642-104647.

15. W. Zhou, Z. Lin, G. Tong, S. D. Stoyanov, D. Yan, Y. Mai and X. Zhu, *RSC Adv.*, 2016, **6**, 111406-111414.

16. X. Tong, H. Zhuo, S. Wang, L. Zhong, Y. Hu, X. Peng, W. Zhou and R. Sun, *RSC Adv.*, 2016, **6**, 34261-34270.

17. H. Xu, *RSC Adv.*, 2016, **6**, 112576-112580.

18. Z. Zapata-Benabithe, F. Carrasco-Marín and C. Moreno Castilla, *J. Power Sources*, 2012, **219**, 80-88.

19. Z. S. Wu, Y. Sun, Y. Z. Tan, S. Yang, X. Feng and K. Mullen, *J. Am. Chem. Soc.*, 2012, **134**, 19532-19535.